The Multi-Purpose Bottom Plug (MPBP) as liquefaction risk mitigation at Galataport Project in Istanbul, Turkey.

A. Lucarelli
ITASCA Consulting Group, Inc., Minneapolis, USA

S. Miranda
TREVI İNŞAAT ve MÜHENDİSLİK A.Ş., Istanbul, Turkey

C. Asioli
TREVI SpA, Cesena, Italy

ABSTRACT: This paper presents the principles, procedures and technologies adopted for the design and execution of the Multi-Purpose Bottom Plug (MPBP). This original geotechnical engineering solution has been employed for the deep basement excavation in Karaköy, within the scope of the Galataport Project, Istanbul, Turkey. MPBP consists of a combination of seepage control, ground improvement and load-bearing elements, which have been executed with double-fluid jet grouting, pseudo-elliptical jet grouting and permanent micropiles, respectively. Three-dimensional dynamic analyses, using the new P2PSand-3D constitutive model implemented in *FLAC3D*, were carried out to evaluate the performance of liquefaction hazard mitigation. The paper highlights the importance of employing advanced geotechnical analysis and design software, cutting-edge technologies within the foundation engineering field and state-of-the-art electronic control devices, in parallel with essential human expertise, in order to obtain the desired results in this high-profile project.

1 THE MULTI-PURPOSE BOTTOM PLUG (MPBP)

This innovative geotechnical engineering solution is a combination of seepage control, ground improvement and load-bearing elements (Figure 1), which was adopted to allow the deep excavation within the footprint of demolished buildings in Karaköy, within the scope of the Galataport Project, Istanbul, Turkey (Miranda et al. 2018). Excavation depth was approximately 12.5 m below the working platform (11.0 m below sea level).

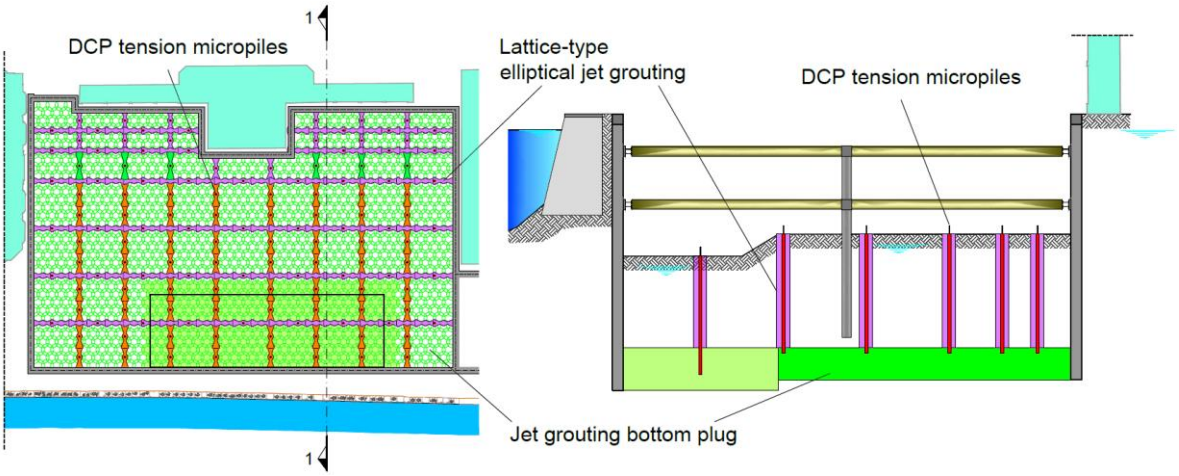

Figure 1. Plan and section view of MPBP.

The main body of the bottom plug is composed of overlapping jet grouting circular columns, executed with the double-fluid method and designed to have a 2,000 mm diameter. Columns are installed in a triangular pattern with an average centre to centre spacing of 1,500 mm. The bottom plug's thickness and depth were designed to ensure the hydraulic stability of the excavation.

Subsequently, pseudo-elliptical jet grouting columns were executed from the top level of the bottom plug up to the excavation level in a lattice-type pattern in order to act as a mitigation element to liquefaction. In particular, the pseudo-elliptical shape of jet grouting columns was chosen instead of a circular one in order to optimize the lattice geometry by minimizing the amount of jetting and related time of execution. The lattice-type jet grouting treatment also acts as a foundation for the future building and will carry the vertical structural loads in permanent conditions. The average width in plan of an elliptical jet grouting column is 4.0 m. Lattice-shaped ground improvements using soil-cement mixtures have been often developed as a solution for liquefaction rick mitigation. The idea is to create a grid of treated soil in order to retain the untreated soil in between and to control its shear deformation during an earthquake, preventing the rising of excess pore water pressure and a possible liquefaction phenomenon.

Finally, the stability against uplift in temporary conditions is ensured by permanent Double Corrosion Protected (DCP) steel bars, which are installed as drilled and grouted micropiles through the previously executed elliptical jet grouting columns. DCP steel bars have a diameter of 63.5 mm and are installed within a 250 mm diameter drill hole (Miranda et al. 2018).

2 NUMERICAL ANALYSIS

2.1 *Geotechnical conditions*

TREVI has executed a few CPTUs to have a better interpretation of the soil conditions in comparison to what was available during the bidding process. The CPTU data have been used to estimate all the parameters necessary for the analysis to support the optimization of the jet grouting cell geometry. Figure 2 shows the typical CPTU profile with the relative density and shear wave velocity.

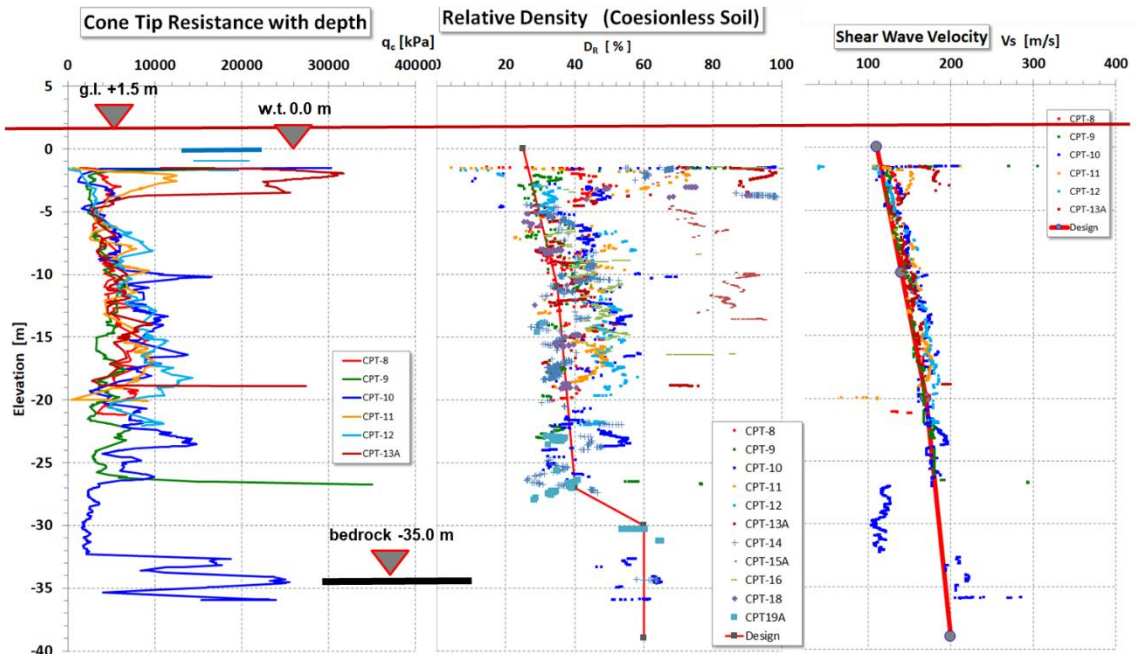

Figure 2. Typical CPTU profile and interpretation.

The profile shows sand with low to medium relative density down to 22-25 m depth. The bedrock is located around 37-38 m depth. In between are a miscellanea of silty-clay layers that will not likely be subject to liquefaction due to some cohesion and relatively high fine content.

Two scenarios are considered for the silty-clay layers, as they might be highly variable inside the footprint: 1) silty-clay modeled as Finn-Byrne material with Darendeli's hysteretic damping not subject to liquefaction; and 2) sand with higher relative density (50-60%) modeled using P2PSand-3D constitutive model.

2.2 *Constitutive model*

The newly developed constitutive model, P2PSand-3D (Cheng 2018), for liquefaction analysis has been adopted. The model is revised based on the original DM04 model developed by Dafalias and Manzari (2004). The modifications implemented leave some elements of the original model intact, such as its conciseness and compatibility with the critical state, the basis on the bonding surface theory, and the fabric-dilatancy related plasticity. The modified formulation switches all void-ratio related formulas into relative-density related formulas (including elastic modulus, plastic-hardening modulus and critical state), improving the matches between the laboratory and field data with the numerical results. The modified version embraces an easier calibration procedure in term of in-situ data (such as blow counts) instead of relaying only on laboratory data (which are quite difficult to obtain). The model improves cyclic performances against the DM04 model, including the following:

1) The slope of the relationship of CRR versus the number of uniform cycles is in a reasonable range, overcoming the overly steep slope predicted by the DM04 model.
2) The shear strain is continuously increasing even after liquefaction occurs, overcoming the shortcoming of the DM04 model, which may fall into a repeated stress-strain loop without further shear strain increase.
3) Compared with the overly large damping ratio at large shear strain calculated from the hysteresis, the corresponding damping ratio is now in a reasonable range.
4) The effect of initial overburden stress fits well with the empirical relation, while the DM04 model has almost no such effect. All the performance improvements only slightly add complexity to the formulations.

2.3 *Seismic input*

Five different time histories have been considered for the liquefaction triggering evaluation: Kocaeli, Tabbas, Mendocino, Irpinia and Loma Prieta. However, just the results related to Kocaeli and Tabbas earthquakes are presented. All motions are considered to be outcrop motions and are directly applied to the base of the numerical models in the horizontal direction only.

2.4 *Natural soil*

A 2 m x 2 m 1D soil column has been modeled for the liquefaction triggering analysis. The size of the mesh, 0.5 m x 0.5 m, is adequate for a correct wave propagation. The fundamental input parameters of the P2D model are relative density and shear wave velocity according to the profiles presented in Figure 2.

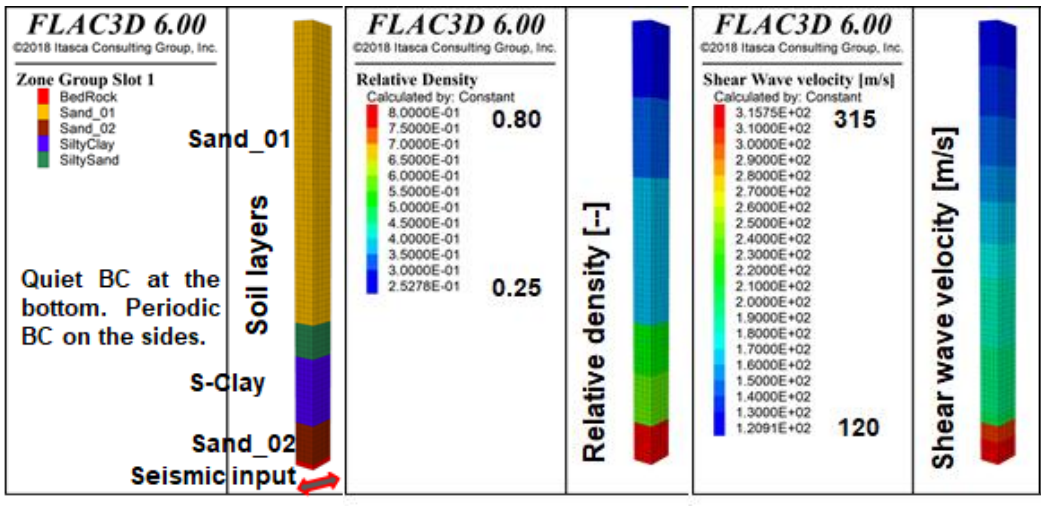

Figure 3. 1D Soil column.

The seismic time history is transformed into a shear stress history applied at the bottom of the model (bedrock). The bedrock is assumed elastic with a shear wave velocity of 750 m/s and a natural density of 2.1 ton/m^3. Therefore, the stress history applied at the bottom is $\sigma_s = \rho \cdot C_s \cdot V_s$. The pore pressure ratio (defined as $r_u = \Delta U/\sigma'_{min}$) is tracked during the analysis for each zone in the model. The analyses have been carried out also considering a small amount of Rayleigh damping (0.2% at 0.5 Hz) to remove high frequency noise. There is a significant impact on the timestep of almost one order of magnitude (7.8e-05 without RD and 1.5e-5 with RD). The analyses have been repeated using a small amount of local damping (3%), instead of RD without any impact on the timestep, this obtains very similar results in terms of velocity, displacements and pore pressure generation. Figure 4 shows the results obtained for the scenario 1. The comparison between the input and the response in terms of velocity shown that the velocity at the bottom was perfectly overlapping the input. This was made to check the behavior of the quiet boundary conditions.

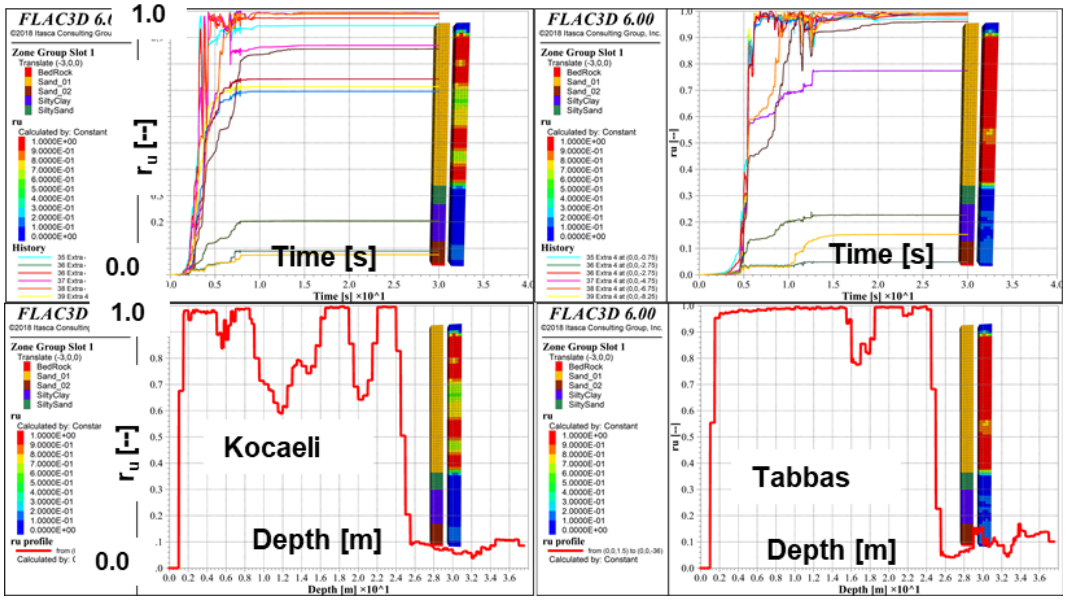

Figure 4. 1D Soil column: Liquefaction triggering analysis, scenario 1.

Figure 5 shows the results obtained for the scenario 2. In this case, stronger motions like Tabbas, Mendocino and Loma may produce localized liquefaction even below 25 m of depth (considering a relative density variable between 50% and 60%, and a friction angle of 34°).

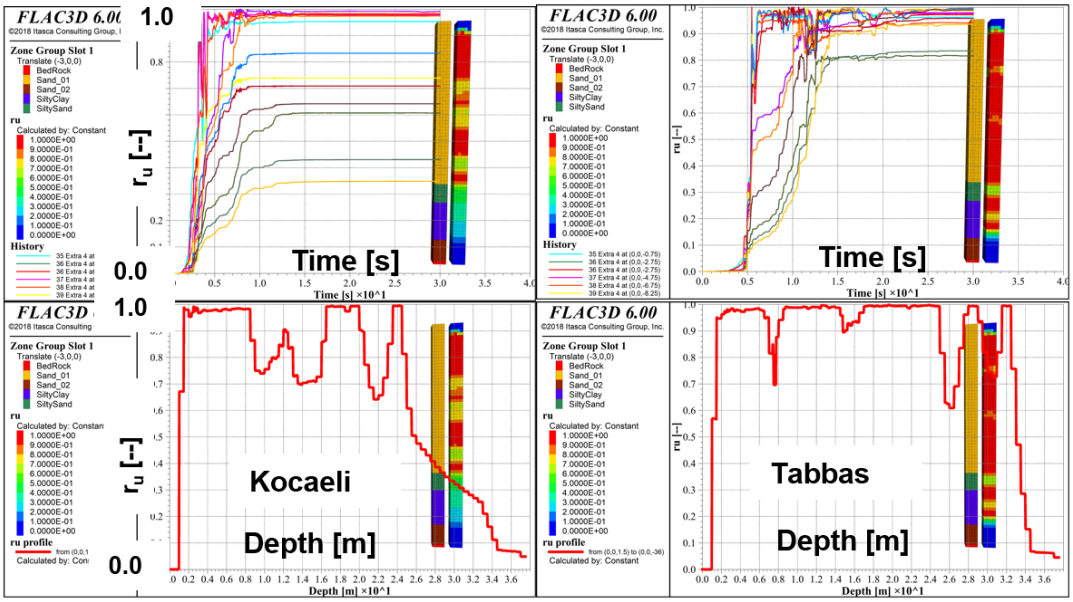

Figure 5. 1D Soil column: Liquefaction triggering analysis, scenario 2.

2.5 *Improved ground response.*

Three sizes of cells have been analyzed: 1) 5 m x 5 m (base solution); 2) 7 m x 7 m (alternative proposed by TREVI); and 3) 10 m x10 m (for sensitivity analysis). The effect of a bottom-plug has also been considered. Finally, for circumstances where there is no significant excavation, an alternative with the treatment extended up to the ground level has also been checked (no bottom plug in this case). The time history considered for these analyses is Kocaeli. The zone size is the same as for the 1D column analysis (0.5 m x 0.5 m). The jet grouting is modeled as Mohr-Coulomb material considering an elastic modulus of 5e6 kPa, cohesion 1300 kPa, zero tensile strength, with density and friction being the same as the original soil. At the bottom of the excavation, a total pressure in equilibrium with the external water table has been applied.

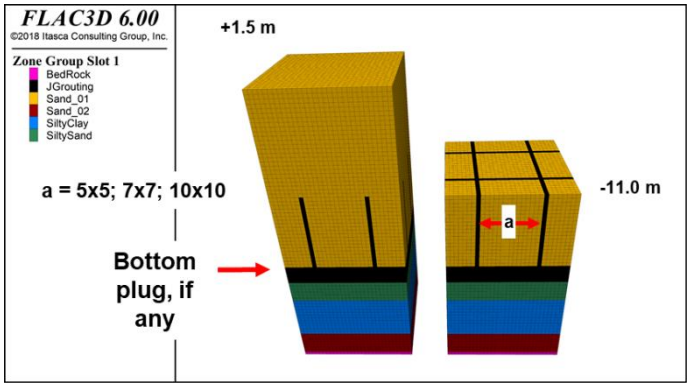

Figure 6. Treated soil geometry.

Figure 7 shows the pore pressure ratio for the three cell sizes considered without bottom plug. The ratio, on average, increases with the cell size as expected. The 10 m x 10 m case looks clearly unacceptable. The 7 m x 7 m case shows very localized values that are reaching 1.0 because of low confinement at the top and the localized shear stain amplification at the bottom. The concentration of shear strain at the bottom is observed for the 5 m x 5 m cells as well, with a ratio around 0.8 (bottom part of the figure shows the r_u profile at the center and at the boundary of the cell).

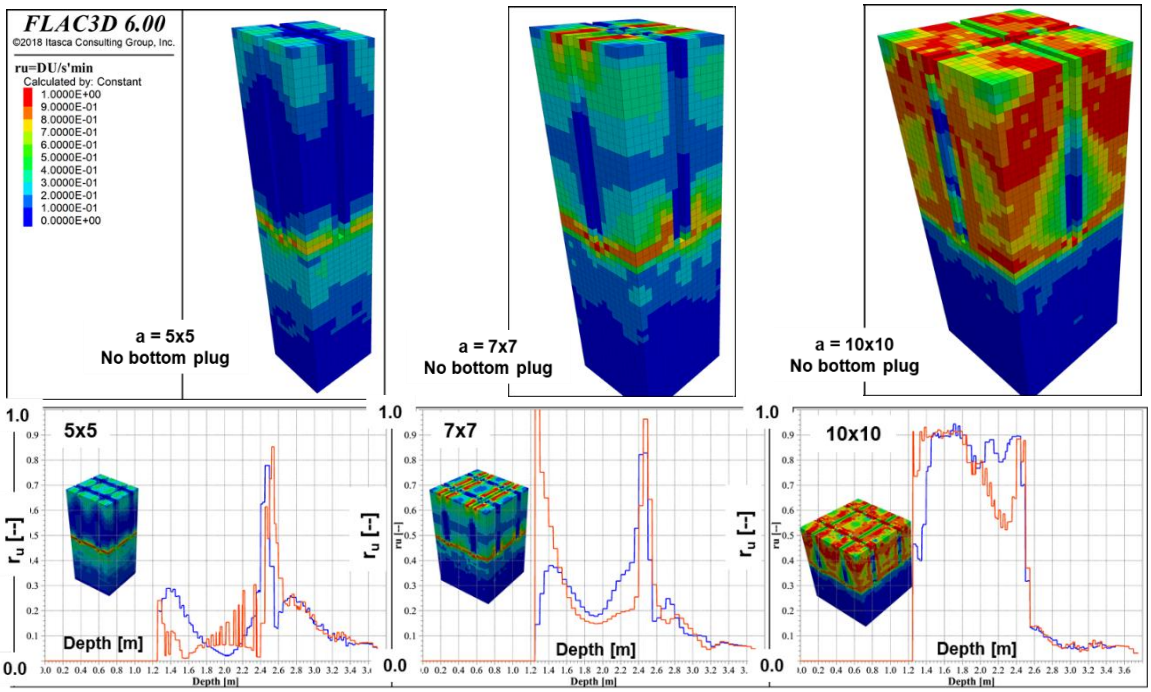

Figure 7. Pore pressure ratio (top part) and pore pressure profiles (bottom part) — no bottom plug.

Figure 8 shows the situation for the bottom plug case, with similar pore pressure ratios at the top as in the case of no bottom plug. The concentration of strain at the bottom of the treated column is not observed anymore.

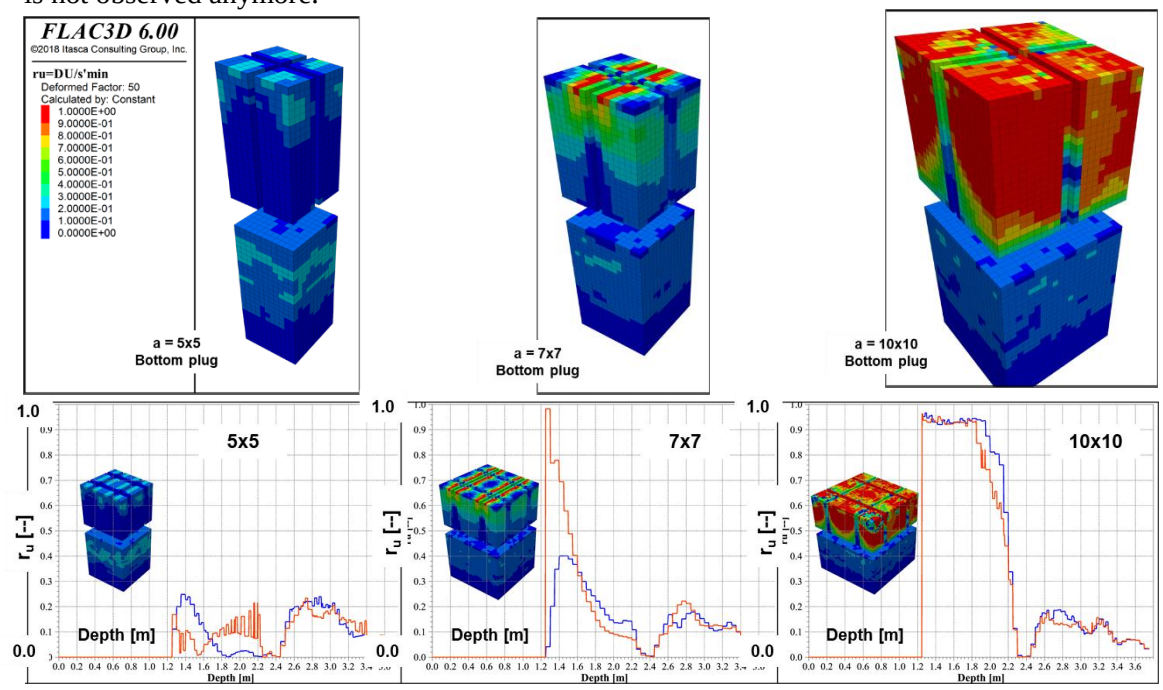

Figure 8. Pore pressure ratio — bottom plug.

It is also interesting to notice in Figure 9 that the pore pressure ratio tends to increase under the bottom plug due to the development of more shear strain and reflection back due to the stiffness modification provided by the treated material. The ratio goes from 0.1 to 0.2 for the Kocaeli time history regardless of the bottom plug. It is not a concern for the stratigraphy 1 scenario, but it might become a factor in case the material under the treated depth is borderline in terms of liquefaction potential.

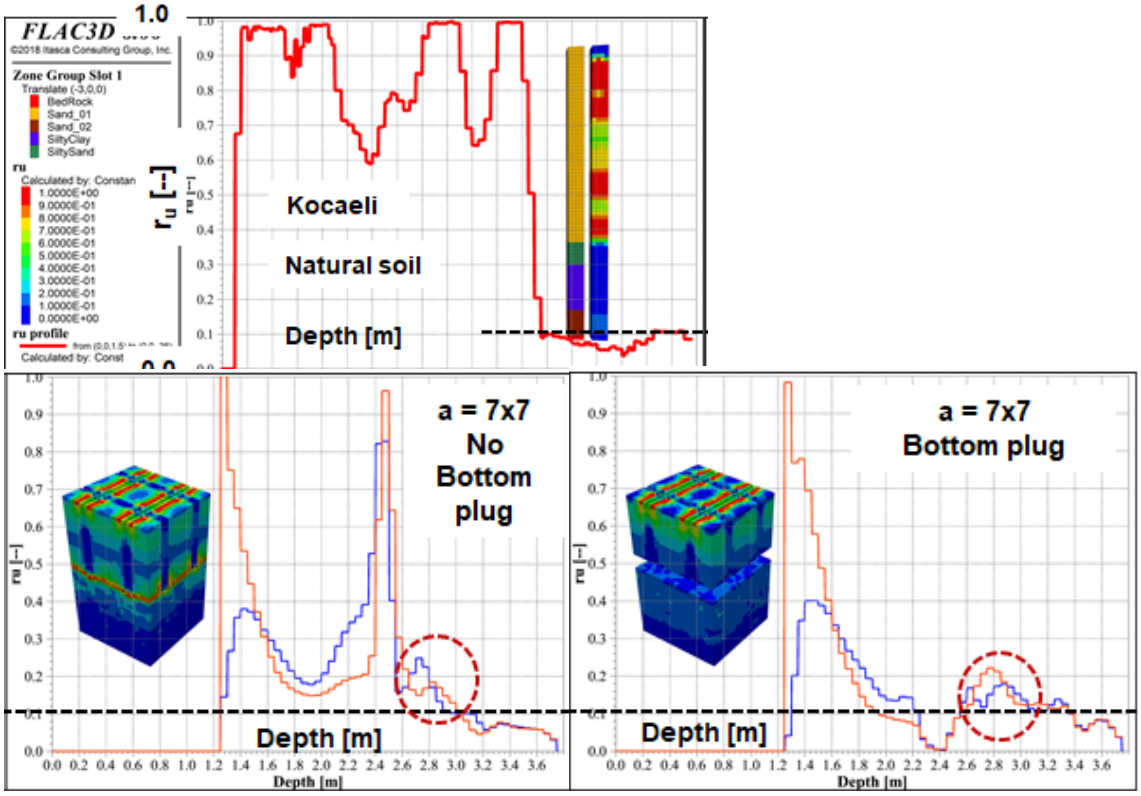

Figure 9. Pore pressure ratio under the treated volume — stratigraphy 1.

In fact, Figure 10 shows the response observed for stratigraphy 2. The 1D soil column analysis was not showing liquefaction for depths greater than 24 m. There is clearly a significant thickness that would liquefy under the treated volume regardless of the bottom plug and the size of the jet grouting cells. This potential outcome might be manageable in the case of flat ground configuration, but it may require more attention in a sloping ground.

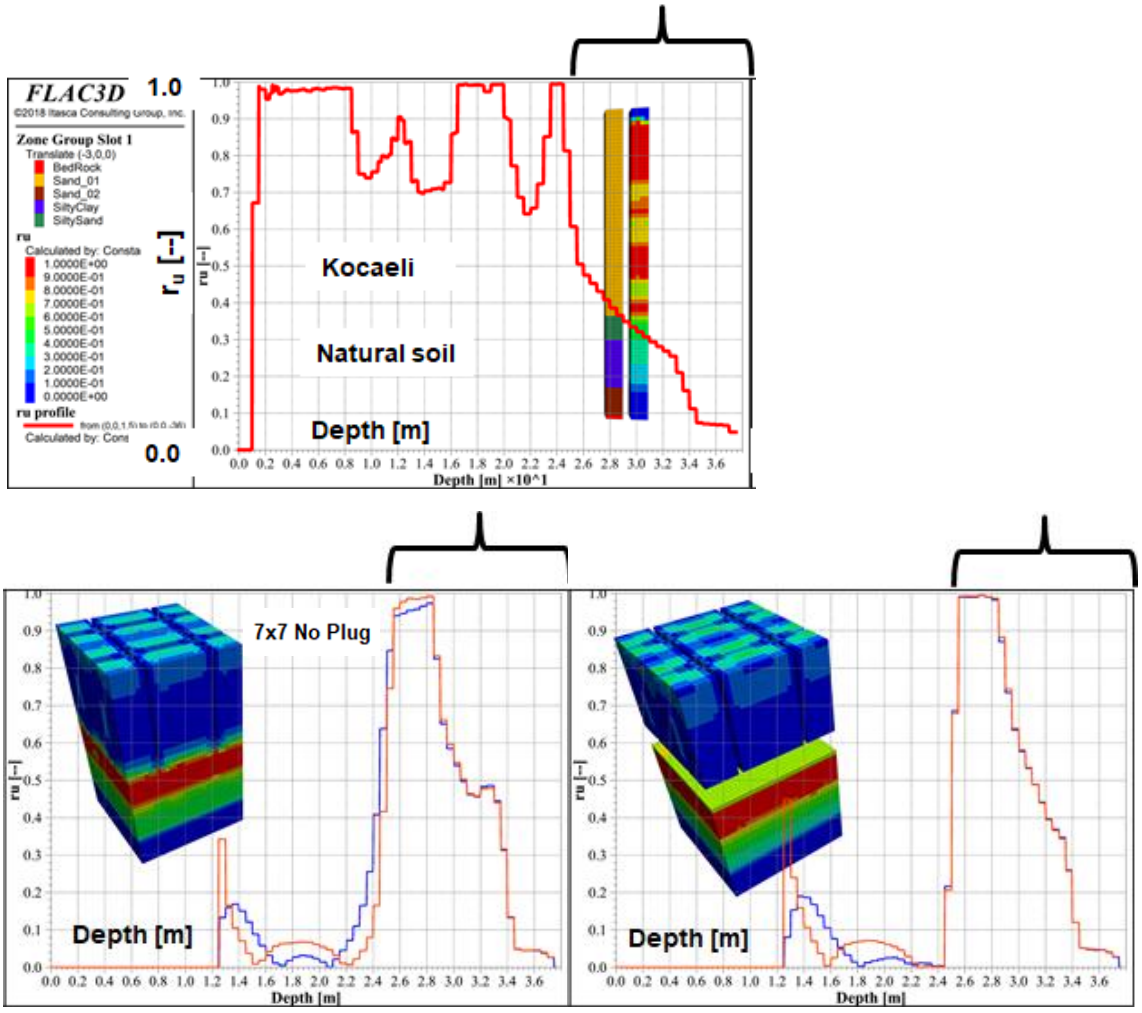

Figure 10. Pore pressure ratio under the treated volume — stratigraphy 2.

Figure 11 shows the results for a 7 x 7 cell considering a stratigraphy of 2. Like the case with a deep excavation shown in Figure 10, there is a significant risk of inducing liquefaction under treatment for a thickness of about 2-3 m.

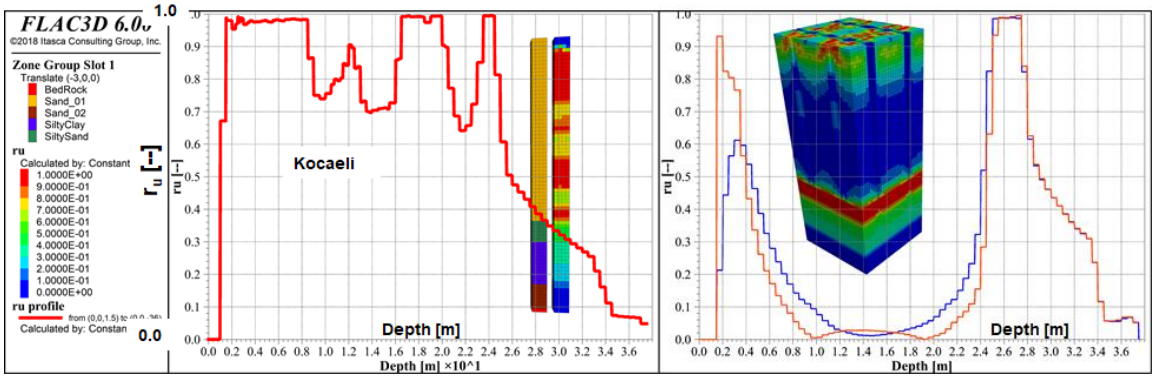

Figure 11. Full-high treatment — 7 x 7, stratigraphy 2.

Finally, a situation with the treatment extended close to the original ground level without a significant excavation is also presented. Figure 12 shows the pore pressure ratio for a 5 m x 5 m and a 7 m x 7 m cell. We observe a similar pattern for the ratio inside the cell, with a tendency to concentrate strains at the top and bottom of the treatment.

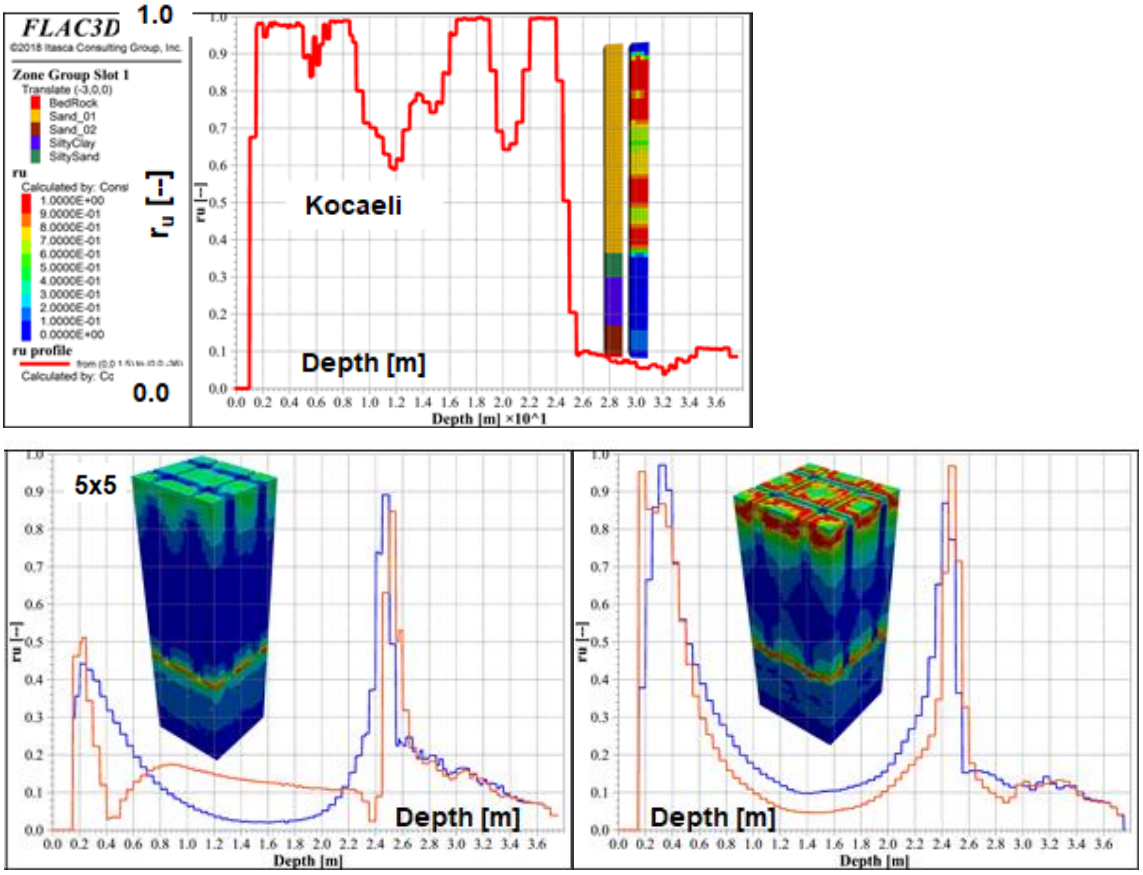

Figure 12. Full-high treatment — 5 x 5 and 7 x 7, stratigraphy 1.

3 CONCLUSION

This paper illustrates the performance of jet-grouting cells for liquefaction hazard mitigation. Three different cell sizes have been considered: 5 m x 5 m, 7 m x 7 m and 10 m x 10 m. The newly developed P2PSand-3D constitutive model implement in *FLAC3D* has been adopted to perform the numerical analyses. The model is a revision of the original DM04 model developed by Dafalias and Manzari (2004). The Galataport Project in Turkey has provided the background to carry out numerous analyses and investigate several scenarios in terms of stratigraphy and geometry. The analyses have shown that increasing the cell size from 5 m x 5 m to 7 m x 7 m would not compromise the performance of the treated volume and would allow for significant optimization of costs and time, but the 10 m x 10 m cell would not be acceptable. The analyses have also shown that the modification of stiffness and strength of the treated material may increase the excess pore pressure distribution underneath the cell (in comparison to the case without treatment). This aspect may require careful evaluation in the case of sloping ground. The reduction of effective stress, even if liquefaction is not developed, may induce large deformation and/or global instability. The increase in excess pore pressure underneath the treated volume is observed for every cell size and it does not seem to be influenced by the high of the cell.

REFERENCES

Miranda, S. Asioli, C. Pagliacci, F. & Chiarabelli, M. (2018) “Galata Port Project in Istanbul: Rehabilitation and restoration works of the terminal for cruise ship and historical surrounding area.” in *Proceedings of the International Foundations Congress and Equipment Exposition (IFCEE 2018, Orlando, Florida USA).*

Dafalias, Yannis F., and Majid T. Manzari. (2004) "Simple plasticity sand model accounting for fabric change effects." *Journal of Engineering mechanics* 130.6 (2004): 622-634.

Cheng, Z. (2018) “A Practical 3D Bounding Surface Plastic Sand Model for Geotechnical Earthquake Engineering Application,” in *Proceedings, Geotechnical Earthquake Engineering and Soil Dynamics V: Numerical Modeling and Soil Structure Interaction (Austin, Texas, June 2018),* pp. 34–47. S.J. Brandenberg and M.T. Manzari, Eds. ASCE.

Itasca Consulting Group, Inc. (2017) *FLAC3D — Fast Lagrangian Analysis of Continua in Three Dimensions* (Version 6.0). Minneapolis: Itasca.